Effect of Melt Annealing on the Morphology and Properties of Polycarbonate Blends

T. W. CHENG, H. KESKKULA, and D. R. PAUL*

Department of Chemical Engineering and Center for Polymer Research, University of Texas, Austin, Texas 78712

SYNOPSIS

The effect of quiescent annealing for brief periods at melt-processing temperatures (e.g., 270°C) were designed to simulate certain conditions that can occur during molding or extrusion. It was found that significant changes in the phase morphology of polycarbonate-based blends can occur in less than 2 min under these conditions. Such morphological rearrangements are detrimental to the mechanical properties of multiphase blends of polycarbonate with rigid polymers, viz., polystyrene, poly(methyl methacrylate), and styrene/acrylonitrile copolymers and core-shell impact modifiers.

INTRODUCTION

The morphology of immiscible polymer blends is an important factor in determining their end-use performance.[1] The morphology developed during processing depends on the type of mixing device, interfacial tension between the phases, rheological characteristics of the components, processing conditions, etc. [1-6] and reflects a dynamic balance between phase deformation or break-up caused by the stresses imposed and phase coalescence or rearrangement driven by the tendency to minimize surface energy. When a molten blend is in a quiescent or low-stress state, e.g., in a mold cavity, a large runner, or a manifold, this dynamic balance is altered and the morphology may become unstable. That is, phase rearrangement including phase coalescence and growth may occur.[7-10] Since such coarsening of the dispersed polymer phase structure will affect the properties of the blend, it is of interest to know about these changes that can occur in blend systems.

A number of studies have reported the incorporation of polymeric modifiers into bisphenol-A polycarbonate (PC) to improve certain mechanical properties, melt flow, or to reduce cost.[1,11] Effects of melt annealing such blends at temperatures typical of melt processing, however, have not been reported. It is clear that at these temperatures the morphological changes can be rapid; hence, significant changes in mechanical properties may result from molding or extrusion processes that involve holding of the melt in a low-stress or quiescent state for any significant time.

This laboratory has previously reported on aging phenomena in miscible PC blends.[12] More recent work has dealt with thermal aging (near the T_g of PC) of impact-modified PC[13] and property–morphology relationships for ternary blends of PC with various brittle polymers (BPs) and impact modifiers.[14] To further understand the behavior of these blends as influenced by various heat fabrication conditions, this study examines the change in morphology of selected binary and ternary blends of PC that occur during brief periods at melt-processing temperature in the absence of flow or stress.

BACKGROUND

Acrylonitrile-butadiene-styrene (ABS) polymers are commercially used to modify PC for improved melt flow and for increased impact strength of thick sections or at low temperatures. In a recent study, modified PCs were prepared by incorporating an impact modifier and various rigid BP phases into PC using various mixing protocols.[14] Thus, it was possible to control the polymeric additive component

* To whom correspondence should be addressed.

Journal of Applied Polymer Science, Vol. 45, 1245–1263 (1992)
 CCC 0021-8995/92/071245-19$04.00

Table I Prediction of MBS Particle Location in PC/BP Blends[14]

Two-Phase Matrix[a]		$\frac{\gamma_{13} - \gamma_{23}}{\gamma_{21}}$	Morphology	
Polymer 1	Polymer 2		Expected MBS Locus	Experimental Result[b]
PMMA	PC	−1.00	MBS in PMMA (marginally)	MBS in PMMA
PS	PC	0.27	Trapped at 1–2 interface	Trapped at 1–2 interface; some in PC
SAN14.7	PC	−0.38	Trapped at 1–2 interface	MBS in SAN14.7
SAN25	PC	−0.35	Trapped at 1–2 interface	Trapped at 1–2 interface; some in both PC and SAN25 phases
SAN34	PC	1.40	MBS in PC	MBS in PC and trapped at 1–2 interface

[a] MBS in polymer 3.
[b] Blends prepared by simultaneous mixing of the three components to obtain a PC/BP/MBS composition of (60/30/10).

ratios independently, unlike in ABS, where the rubber to brittle polymer phase ratio and morphological structure are fixed.

The choice of polymers was based on a number of considerations. An emulsion-made methacrylated-butadiene-styrene (MBS) core-shell impact modifier was chosen because of the thermodynamic interaction of the poly(methyl methacrylate) (PMMA) shell with PC.[15] The BPs were chosen to have various levels of interactions with PC and with the PMMA shell of the MBS modifier. Polystyrene (PS) is not miscible with either PC or PMMA, while PMMA is more nearly miscible with PC. Styrene-acrylonitrile copolymers (SANs) were chosen that span the whole miscibility range [9–33% acrylonitrile (AN)] with PMMA.[16] With this selection of BP components, a wide range of phase morphologies was anticipated.

The location of methyl methacrylate (MMA)-grafted emulsion rubber particles within the two-phase matrix formed by PC and the BP should theoretically be determined by interfacial forces, at the melt-blending temperature, as described recently.[14] Table I summarizes the location of the MBS particles as predicted by interfacial force considerations and the results found by experiment. Here, we designate the BP as component 1, PC as 2, and the MBS (PMMA shell) as 3. When the interfacial tensions satisfy the inequality

$$\lambda_{12} = \gamma_{23} - \gamma_{13} - \gamma_{12} \geq 0 \qquad (1)$$

Table II Polymers Used in This Study

Polymer	Abbreviation	Source (Designation)	Molecular Weight
Polycarbonate	PC	Dow Chemical Co. (Calibre 300-4)	M_n = 13,400 M_w = 36,000
Poly(methyl methacrylate)	PMMA	Rohm & Haas Co. (Plexiglas V811)	M_n = 52,900 M_w = 105,400
Polystyrene	PS	Cosden Oil and Chemical Co. (550P)	M_n = 100,000 M_w = 350,000
Poly(styrene-co-acrylonitrile)			
14.7% AN	SAN14.7	Asahi Chemical Co.	M_n = 83,000 M_w = 182,000
25% AN	SAN25	Dow Chemical Co. (Tyril 1000)	M_n = 77,000 M_w = 152,000
34% AN	SAN34	Asahi Chemical Co.	M_n = 73,000 M_w = 145,000
Methacrylated-butadiene-styrene impact modifier	MBS	Rohm & Haas Co. (Acryloid KM 680)	Not applicable

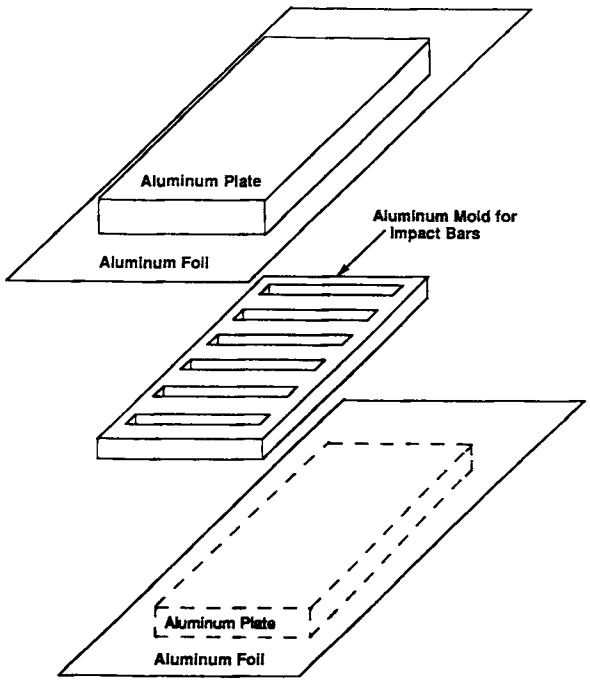

Figure 1 Schematic of the mold configuration used for melt annealing.

the MBS particles or 3 will locate in phase 1 (BP) at equilibrium. When the interfacial tensions satisfy the inequality

$$\lambda_{21} = \gamma_{13} - \gamma_{23} - \gamma_{12} \geq 0 \qquad (2)$$

the MBS particles or 3 will reside in phase 2 (PC) at equilibrium. In eqs. (1) and (2), the γ_{ij} are interfacial tensions while the λ_{ij} are spreading coefficients.[14,17,18] When the following condition is satisfied

$$-1 < \frac{\gamma_{13} - \gamma_{23}}{\gamma_{12}} < 1 \qquad (3)$$

the particles will be trapped at the 1–2 interface by surface forces[14] when equilibrium prevails.

As noted in Table I, the critical surface tension ratio predicts that the expected MBS particle location is at the PC/BP interface in most cases. For SAN34 and marginally for PMMA as the BPs, the MBS particles are predicted to be in the PC and the PMMA phases, respectively.

Based on these predictions and reported experimental observations, it is of interest to experimentally examine any morphological changes that occur during melt annealing at temperatures typically used for fabrication of PC blends.

EXPERIMENTAL

The materials used in this study are listed in Table II. They are all commercially available polymers. An emulsion-made MBS core-shell impact modifier, available from Rohm and Haas under the trade name Acryloid KM 680, was used for toughening. It contains about 80% by weight of a butadiene-based rubber and consists of 0.18-μm diameter particles that have a PMMA-based outer shell. More details of this rubber modifier have been given elsewhere.[19] The following BPs were used: PS, PMMA, and a series of SANs of varying AN contents.

PC was dried for a minimum of 24 h at 105°C in an air-circulating oven while the various BPs and MBS modifier were dried at 75°C. Melt blending was carried out in a Killion single-screw extruder (D = 1 in, L/D = 30) at 270°C. The single-strand extrudate was pulled through a water bath and pelletized. All ternary blends, PC/BP/MBS, used here were prepared by simultaneous mixing (one pass through extruder) to obtain the fixed composition of (60/30/10), while binary blends had variable compositions. The blended pellets were dried at 100°C overnight prior to molding into Izod bars (ASTM-256) in an Arburg Allrounder 305 screw-type injection-molding machine whose barrel temperature was set at 270°C.

Injection-molded bars were dried at 100°C overnight in a convection oven prior to carrying out the

Table III Effect of Melt Annealing on Izod Impact Strength (ft-lb/in) of PC and Its Blends

Material	As-Molded	Melt Annealed at 270°C		
		2 Min	10 Min	30 Min
PC	17.6	17.2	18.0	17.5
PC/MBS (90/10)	13.8	13.4	14.3	13.7
PC/MBS (80/20)	9.5	9.2	8.9	7.6
PC/PS (80/20)	2.0	0.5	0.4	0.2
PC/SAN25 (70/20)	1.3	1.1	0.9	0.8
PC/PMMA (60/30)	1.1	1.0	0.9	0.8
PC/PS (60/30)	0.6	0.4	0.2	0.2
PC/SAN25 (60/30)	1.1	0.8	0.7	0.6
PC/PMMA/MBS[a]	8.9	6.0	3.3	2.4
PC/PS/MBS	2.3	1.4	1.2	0.8
PC/SAN14.7/MBS	7.3	1.6	1.3	1.2
PC/SAN25/MBS	8.7	1.6	1.2	1.0
PC/SAN34/MBS	6.9	0.9	0.8	0.8

[a] Composition of all ternary blends is (60/30/10) and they were prepared by simultaneous mixing of all components in a single-screw extruder.

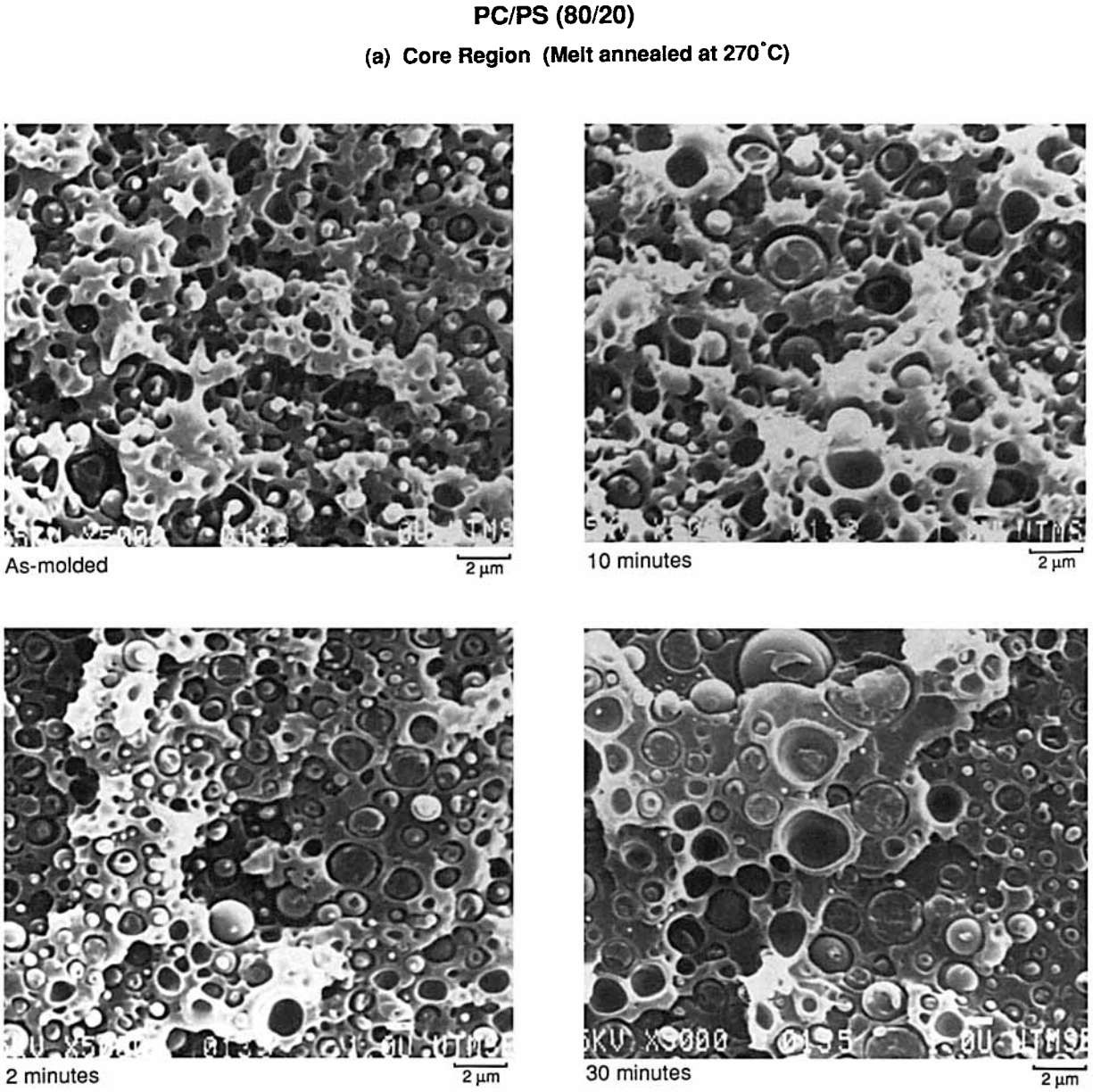

Figure 2 SEM photomicrographs of fracture surfaces of PC/PS (80/20) blends for various melt-annealing times at 270°C. (a), core region; (b), skin region.

melt-annealing experiment. The dried bars were wrapped firmly with aluminum foil, then fitted into slots of a aluminum mold that was subsequently covered with aluminum foil and metal plates as shown schematically in Figure 1. Since the processing temperature for melt blending was set at 270°C, the covered bars were annealed as a function of time at 270°C in a compression press that imposed a force of 620 psi on the mold assembly illustrated in Figure 1.

Prior to adoption of the above-mentioned approach, molded bars covered with aluminum foil were placed directly in an air convection oven set at 270°C. It was found that there was significant expansion of the specimen dimensions and concurrent formation of voids that made this method unacceptable. Even using the preferred technique of annealing in a mold under pressure, some voids developed in the specimens. While satisfactory notched Izod measurements could be made, attempts to obtain tensile properties frequently resulted in premature failure caused by voids.

Notched Izod impact strengths were measured according to ASTM D-256 using a pendulum type

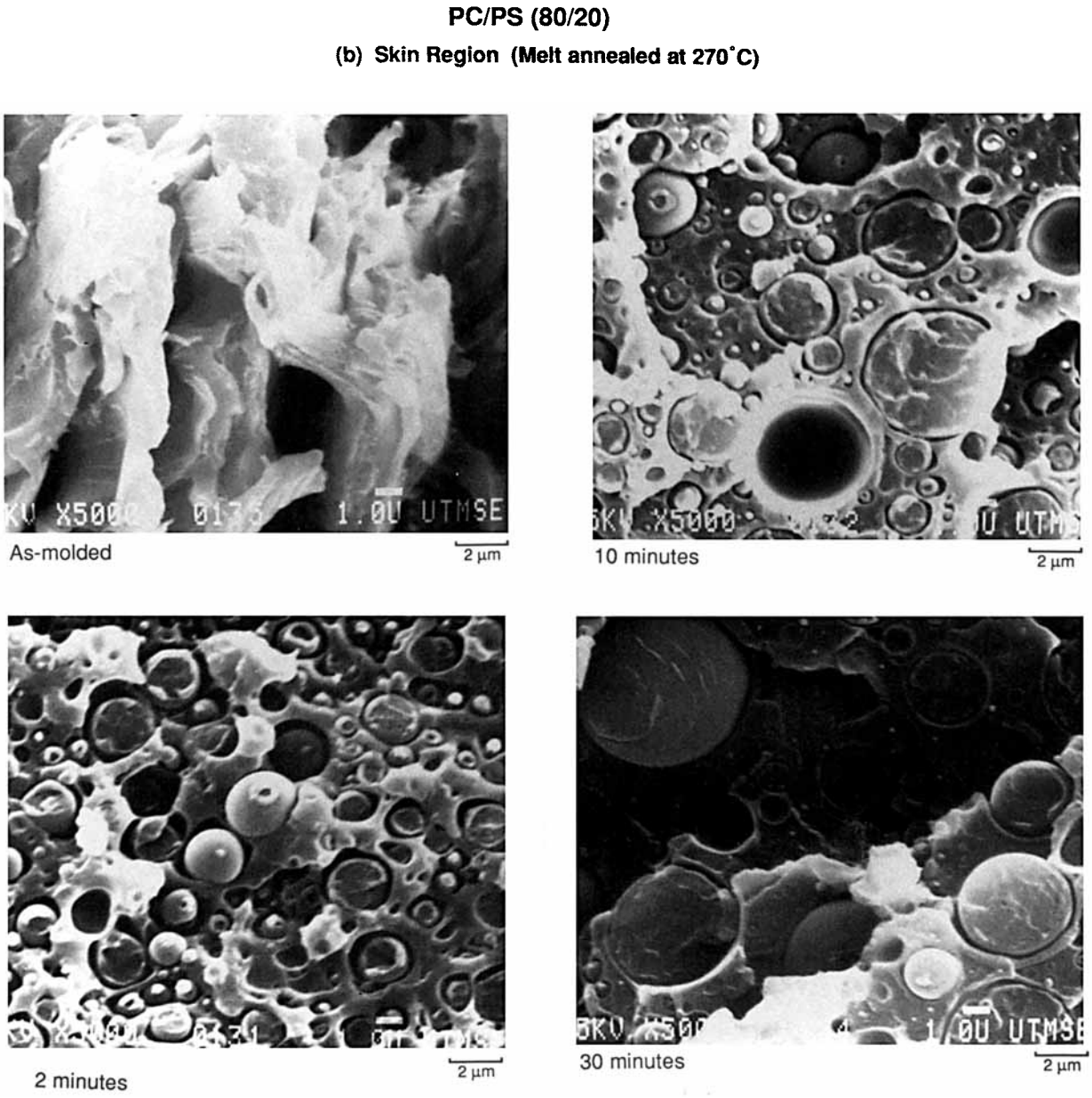

Figure 2 (*continued from previous page*)

tester. A minimum of five bars were tested for each data point reported. The standard deviation for Izod impact values was found to be about 5%.

Thermogravimetric analysis (TGA) was carried out on a Perkin-Elmer TGA-7 unit. Samples were heated in nitrogen at 40°C/min to 270°C and isothermally annealed for 30 min, then subsequently heated at a rate of 10°C/min up to 600°C.

Dynamic mechanical properties at 3 Hz were measured in the single-cantilever bending mode by a Polymer Laboratories DMTA at a heating rate of 2°C/min. The specimen cross-section was 12 × 3 mm^2 with a span of 8 mm.

Blend phase morphology was examined by transmission (Hitachi HU11-E, TEM) and scanning electron microscopy (JEOL JSM-35C, SEM). For the TEM observations, sample blocks of ternary blends cut from injection-molded bars were stained in a water solution of 2 wt % osmium tetroxide (OsO_4) for at least 48 h. Ultrathin sections were cut using a Reichert-Jung Ultracut Microtome at room temperature. Phase contrast was enhanced by sub-

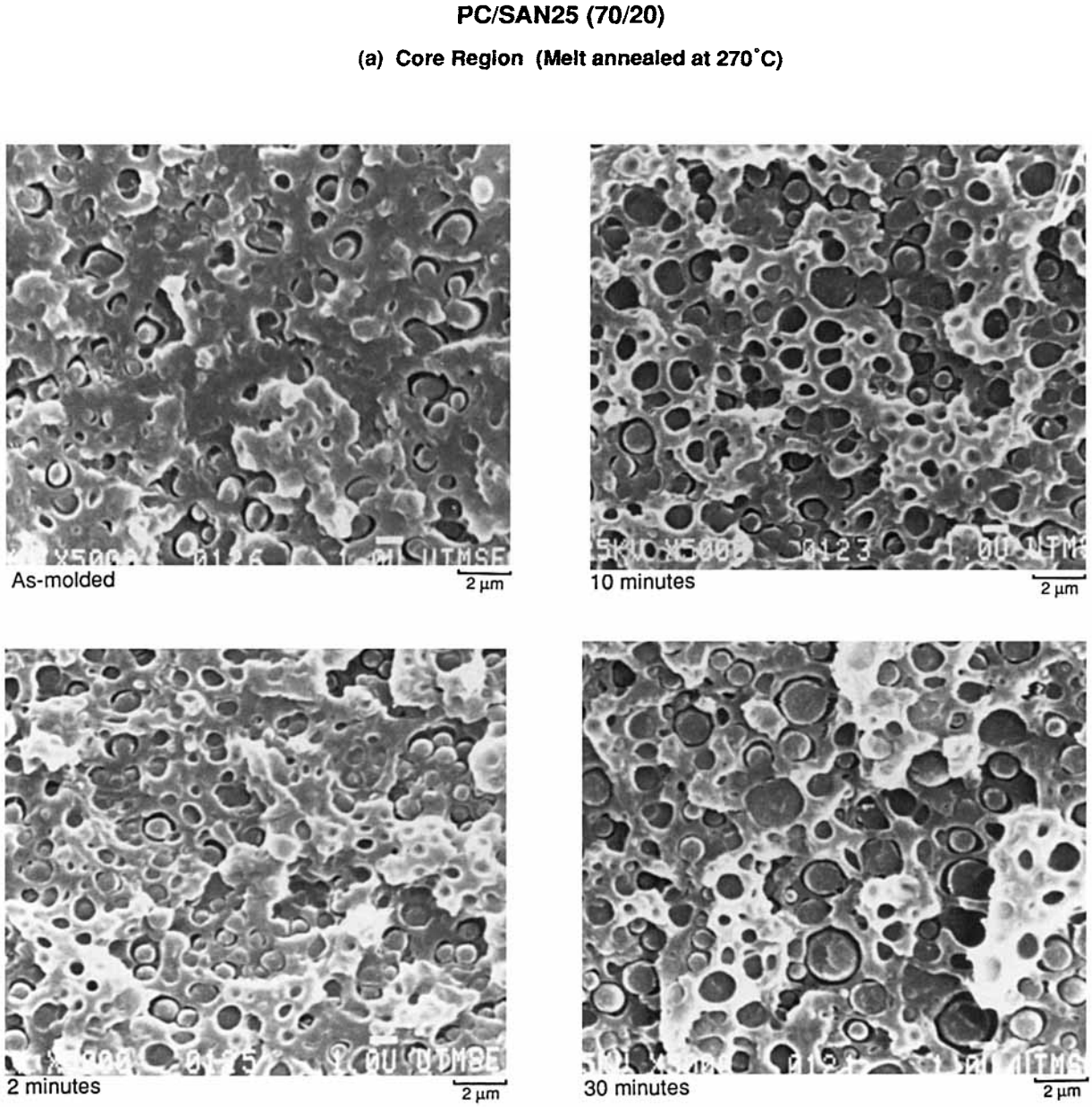

Figure 3 SEM photomicrographs of fracture surfaces of PC/SAN25 (70/20) blends for various melt-annealing times at 270°C. (a), core region; (b), skin region.

sequent exposure of these sections to the vapor of an aqueous solution of 0.5 wt % ruthenium tetroxide (RuO_4) for a maximum of 15 min.[20] In most cases, the binary blends were only stained by RuO_4. Microtomed sections were cut perpendicular to the flow direction. Fracture surfaces created in a notched Izod test at room temperature were used for SEM observation. In some cases, SEM observations were made after removal of the PC phase from a polished surface by etching with a 30 wt % aqueous solution of sodium hydroxide[21] for 20 min at 60°C to develop phase contrast. Prior to SEM examination, all surfaces were coated with gold/palladium (60/40) using a Pelco Model 3 Sputter Coater, then viewed at a beam voltage of 25 kV. Surface polishing was accomplished using the microtome with a glass knife.

IZOD IMPACT STRENGTH

Table III summarizes the effect of melt annealing on notched Izod impact strength of PC and its

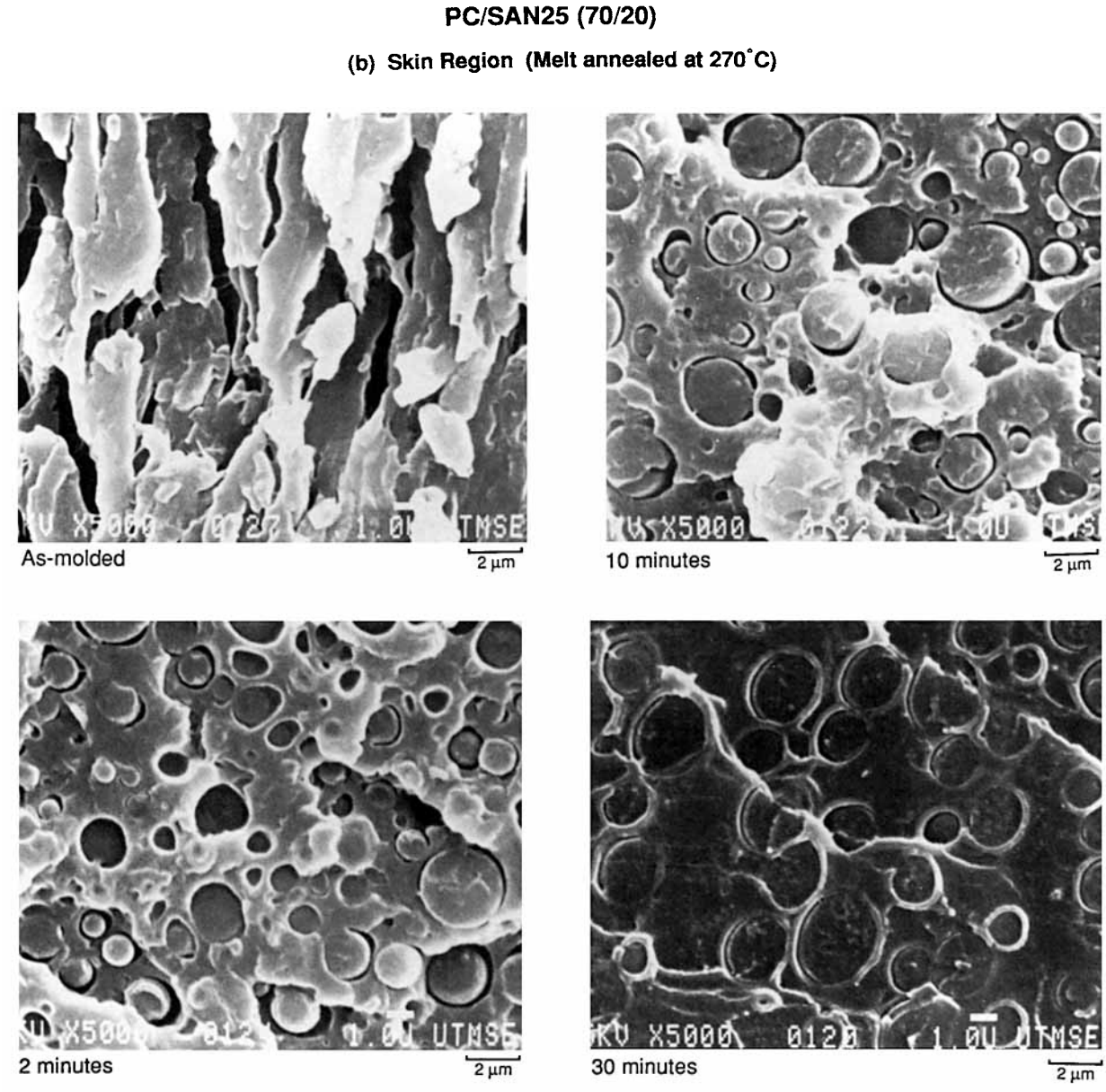

Figure 3 *(continued from previous page)*

blends. As expected, melt annealing has no effect on the Izod impact strength of neat PC. For PC blends with MBS, the 90/10 composition gives excellent Izod values for up to 30 min of exposure at 270°C, but the impact strength of the 80/20 blend is reduced somewhat by continued melt annealing. For binary blends of PC with the various BPs, the impact strength decreases with melt annealing time. For ternary PC/BP/MBS (60/30/10) blends, a significant reduction of impact strength was observed after melt annealing at 270°C for only 2 min. The loss of impact strength is more gradual and moderate for the ternary blend containing PMMA. This result is interesting since PMMA should be less thermally stable at 270°C than the various styrenic polymers used. Evidently, other factors must be responsible for the sharp loss of impact strength of ternary blends after only 2 min of exposure at 270°C.

MORPHOLOGY

SEM and TEM were used to characterize blend morphology. For PC blends containing 30% or more of the BPs, it has been observed that the dispersed

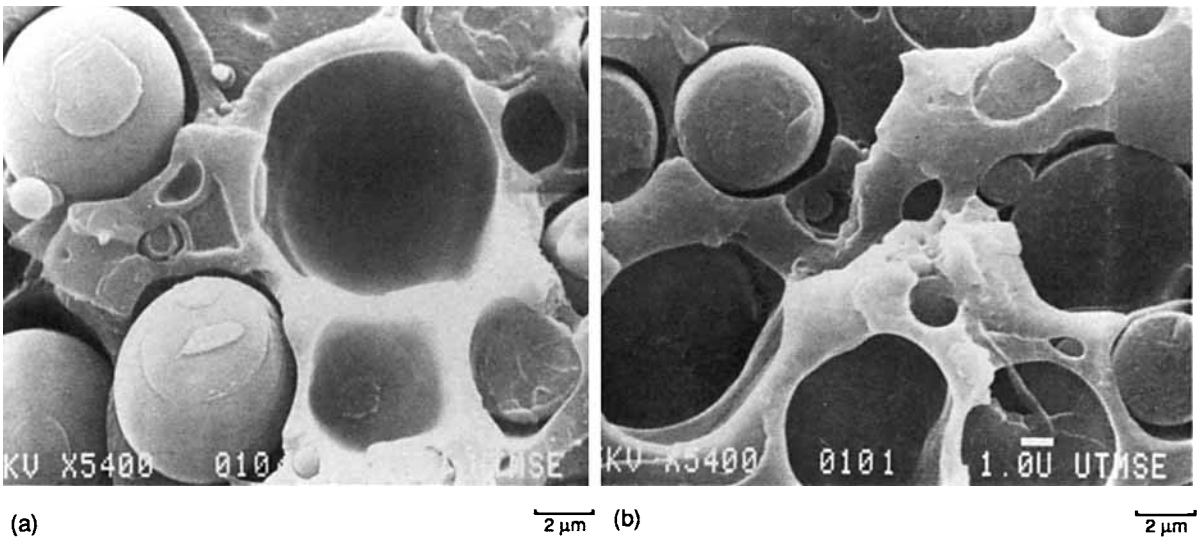

Figure 4 SEM photomicrographs of fracture surfaces of PC/BP (80/20) blends after melt annealing at 260°C for 30 min in an air oven without external pressure. (a), PC/PS; (b), PC/SAN25.

domains tend to have irregular shapes.[5,14,22,23] PC/PS (80/20) and PC/SAN25 (70/20 or 78/22) blends were selected for investigation of domain structural changes during melt annealing. Figures 2 and 3 show SEM photomicrographs of fracture surfaces for PC/PS (80/20) and PC/SAN25 (70/20) blends after various melt-annealing histories. Since injection-molded parts often have an oriented skin layer and a more isotropic core, both these regions were examined by microscopy. As seen in Figure 2(a), the PS domains from the core region of the as-molded samples have diameters under 1 μm. Melt annealing at 270°C causes continuous and appreciable increases in domain size. Even after 2 min of melt annealing, some domains exceed 2 μm in diameter. The as-molded skin region appears to have a multilayer or laminated structure that is formed during molding. As seen from Figure 2(b), this oriented skin layer is dramatically restructured into more typical spherical domains after only 2 min of melt annealing. A similar change in phase morphology also occurs in PC/SAN25 blends as seen in Figure 3. Thus, PS and SAN25 phases in PC show significant growth in domain size with melt-annealing time at 270°C. PS domains appear to grow more rapidly than those of SAN25, and the growth is greater in the skin region for both blends. An even more dramatic increase in BP domain size occurs when melt annealing is carried out without external pressure. Figure 4 shows the change in BP domain size after unconstrained melt annealing at 260°C for 30 min in an air oven. As pointed out earlier, this method of annealing was abandoned because of the excessive swelling of the specimens caused by void formation.

These SEM photomicrographs of PC/BP blend fracture surfaces reveal another important fact: The fracture tends to propagate through the dispersed SAN25 domains in the PC matrix; however, the fracture seems to go around PS particles. Similar conclusions may be reached from Figures 2–4. This indicates better adhesion at the PC–SAN25 interface than at the PC–PS interface, consistent with previous direct measurements of adhesion.[22]

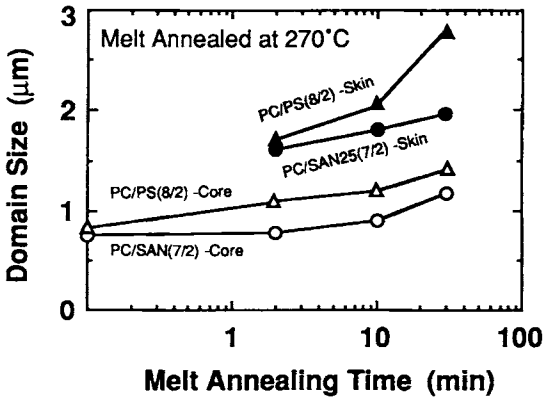

Figure 5 Effect of melt-annealing time at 270°C on growth of domain size of PC/PS (80/20) and PC/SAN25 (70/20) blends.

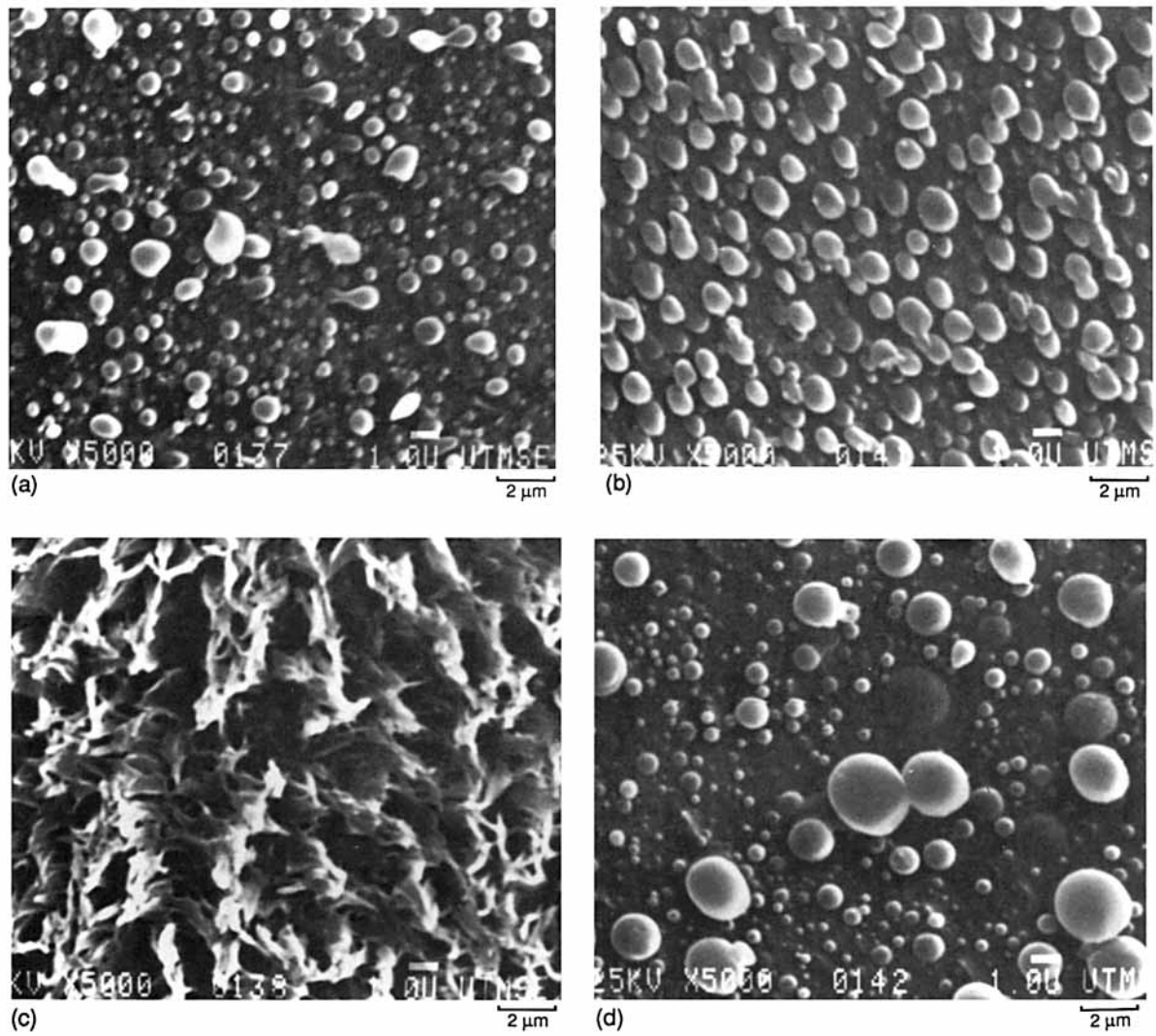

Figure 6 SEM photomicrographs of polished surfaces of PC/SAN25 (70/20) blends after removal of the PC phase using a 30 wt % aqueous solution of sodium hydroxide at 60°C for 20 min. (a), core region of as-molded sample; (b), core region of melt-annealed sample (2 min at 270°C); (c), skin region of as-molded sample; (d), skin region of melt-annealed sample (2 min at 270°C).

To quantify the coarsening of the BP domains in the PC matrix, average effective domain diameters were computed from SEM photomicrographs. Because of the solubility of PC in a number of organic solvents, it is difficult to selectively remove the BP domains that would be necessary to utilize image analysis techniques for a rigorous quantification of particle size. As a practical matter, we arbitrarily chose to count the largest 50 BP domains in each photomicrograph for the calculation of average domain diameters. When the photomicrographs contained less than 50 BP particles, all BP domains were counted. The weight average domain diameter, d_w, was calculated from the definition[24]

$$\bar{d}_w = \frac{\sum n_i d_i^2}{\sum n_i d_i} . \quad (4)$$

This average gives heavier weighting to the larger domains, which means that the pragmatic choice to count only the larger domains does not overly bias the estimate of average domain size. The average domain diameter so obtained is plotted as a function of melt annealing time at 270°C in Figure 5. In this

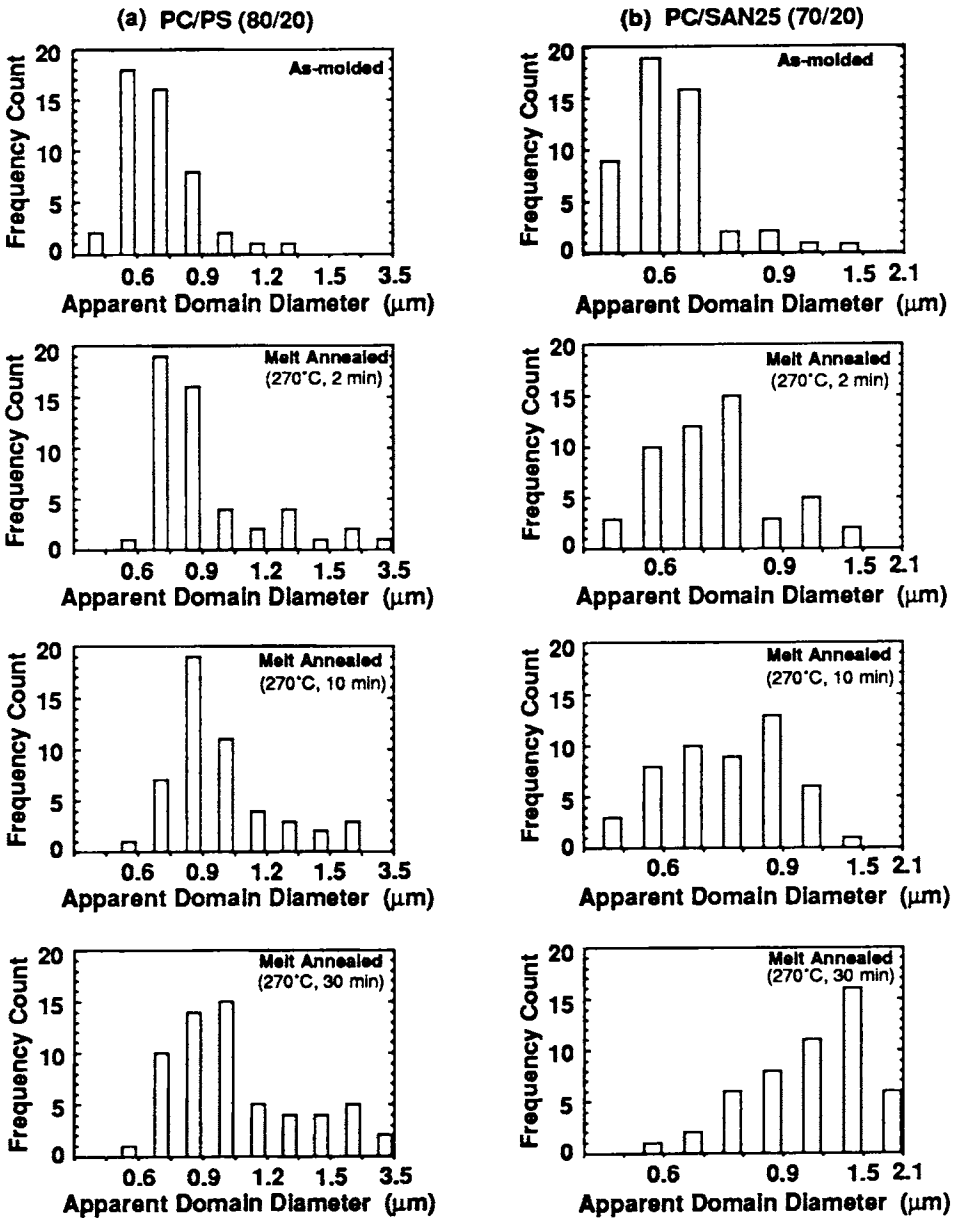

Figure 7 Effect of melt annealing at 270°C on apparent domain size distribution for PC blends. (a), PC/PS (80/20); (b), PC/SAN25 (70/20).

and subsequent plots with a logarithmic time scale, the domain sizes given on the ordinate represent the values for as-molded samples. While PC/PS (80/20) and PC/SAN25 (70/20) blends have similar BP domain sizes before annealing, the PS domains exhibit more growth during melt annealing, probably owing to a higher interfacial tension at the PC–PS interface in comparison to that at the PC–SAN25 interface according to values calculated in a recent report.[14] No initial domain sizes are indicated for the skin regions since the morphology is too complex to be characterized so simply. The multilayer skin structure tends to quickly reorganize to form dispersed domains of larger dimension than found in the core region. This is clearly shown in Figure 3(b), where the complex oriented skin domain structure of PC/SAN25 blend relaxed very rapidly at 270°C, giving rise to large spherical SAN25 particles. Figure

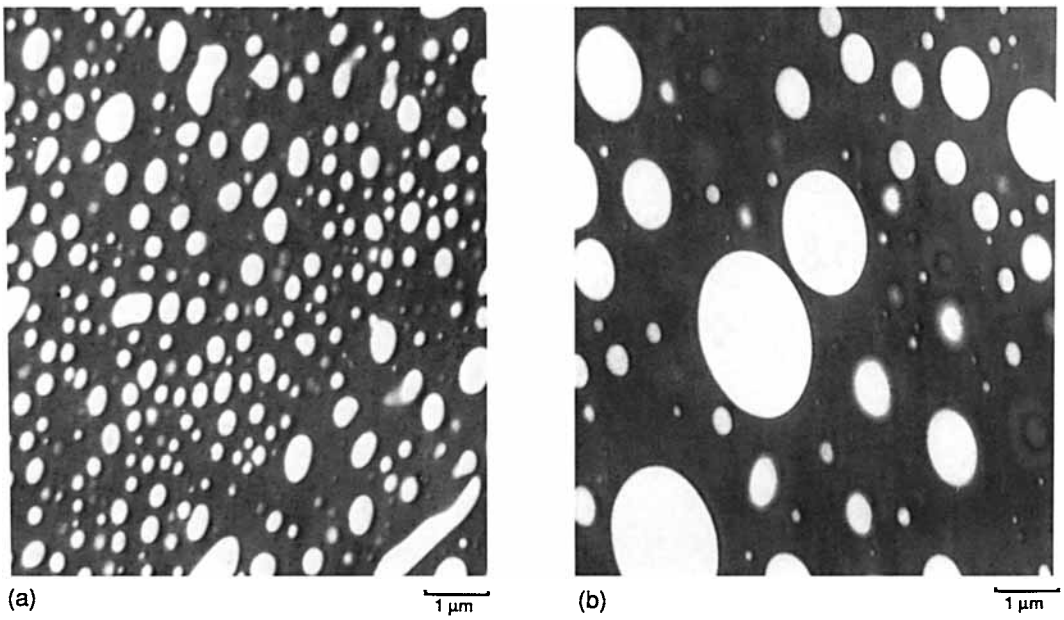

Figure 8 TEM photomicrographs of as-molded and melt-annealed (30 min at 270°C) PC/SAN34 (60/30) blends. Samples were microtomed from injection-molded bars perpendicular to flow direction at room temperature and stained with RuO_4.

6 also shows this transformation for a PC/SAN25 blend via SEM photomicrographs of polished fracture surfaces from which the PC phase has been removed by extraction. Here, the complex cocontinuous skin region [Fig. 6(c)] is relaxed within 2 min to produce spherical SAN25 particles with a broad size distribution. Figure 7 shows how the apparent domain size distribution in the core region changes with melt-annealing time. It is clear that melt annealing at 270°C both increases the average domain dimension and broadens its distribution.

For PC/BP (60/30) blends, both irregular and elliptical shaped domains have been observed in as-molded specimens. However, the BP domains tend to develop into more spherical shapes during melt annealing and, of course, have a much larger size distribution due to domain coalescence. Figure 8 shows a typical comparison of the morphology of a PC/SAN34 (60/30) blend as molded and after melt annealing at 270°C for 30 min.

Figure 9 compares the morphology of as-molded and melt-annealed (at 270°C for 30 min) samples of ternary PC/BP/MBS (60/30/10) blends. PMMA, PS, SAN14.7, SAN25, and SAN34 are the BP components used in these blends, and as mentioned previously were selected because of their interactions with the PMMA graft layer of the core-shell modifier and with PC. While PS and SAN34 are immiscible with PMMA; SAN14.7, SAN25, and PMMA homopolymer should be miscible with the PMMA graft.[16,25] Furthermore, SAN14.7 should have the strongest interaction as judged from the lower critical solution temperature (LCST) of its blends with PMMA.[16] Polycarbonate is on the verge of miscibility with PMMA as shown by recent studies,[15] and its adhesion to styrene-acrylonitrile copolymers is greatest at about 25% AN,[21] which suggests optimal thermodynamic interaction with SAN25 compared to the other styrenic polymers used here. For as-molded ternary blends containing PMMA, SAN14.7, or SAN25, the BP phase tends toward cocontinuity with the PC (darker) phase. For ternary blends involving PS and SAN34, however, the BP phase seems to have about the same shape as found in the corresponding binary blends without the MBS modifier.

After melt annealing at 270°C for 30 min, coarsening and coalescence of the BP domains was observed for all ternary blends. This change reduces the PC–BP interfacial area and tends to cause MBS particles to accumulate at this interface for most of the ternary blends. When PMMA is the brittle polymer, the MBS particles are located within the PMMA phase in the as-molded material and remain there during melt annealing. There is some evidence for agglomeration of MBS particles within the

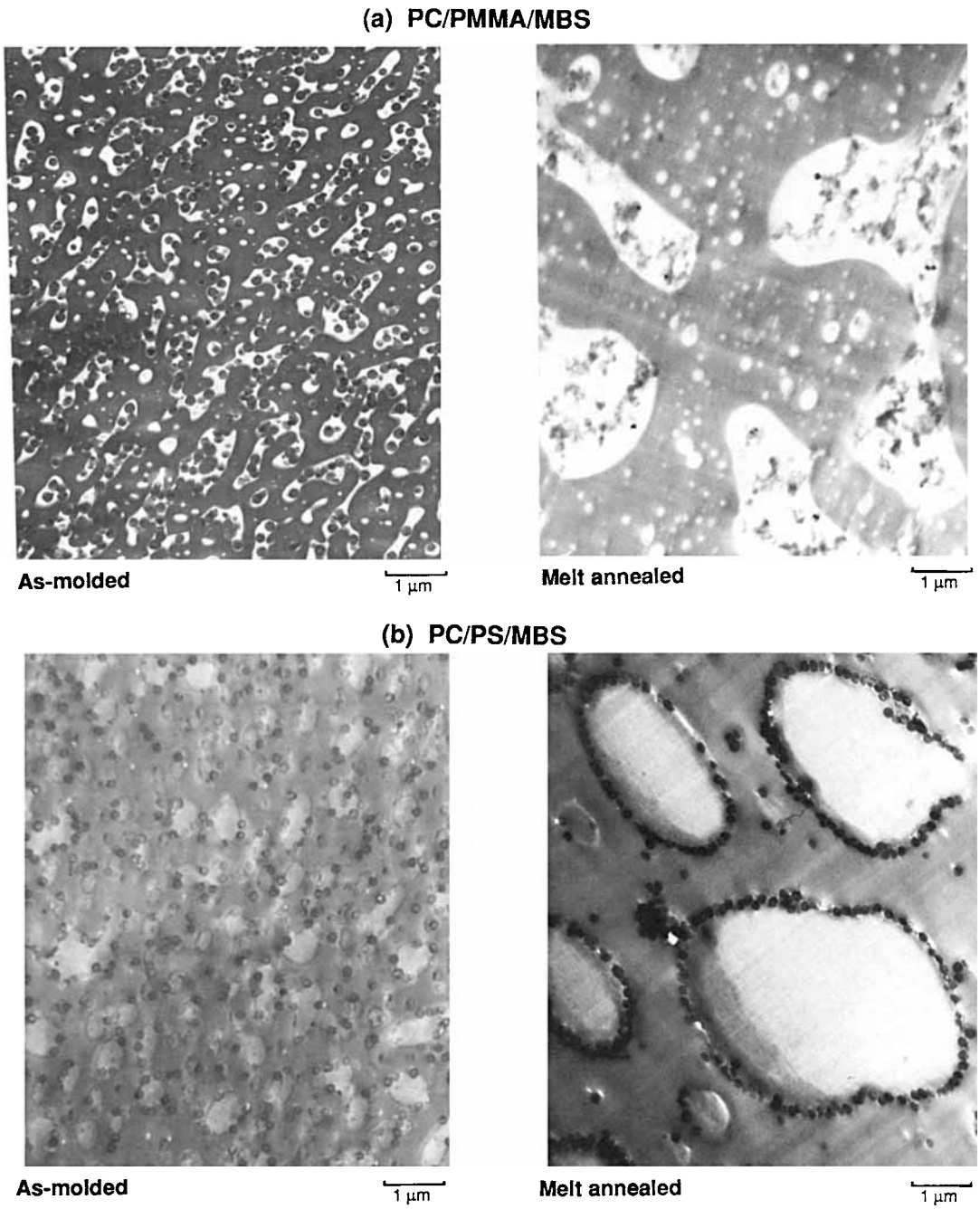

Figure 9 TEM photomicrographs of as-molded and melt-annealed (30 min at 270°C) PC/BP/MBS (60/30/10) blends. Samples were microtomed from injection-molded bars perpendicular to the flow direction at room temperature and stained with OsO_4 and RuO_4. BP: (a), PMMA; (b), PS; (c), SAN14.7; (d), SAN25; (e), SAN34.

PMMA phase during this step as seen in Figure 9(a). The PC and PMMA phases have a strong tendency for cocontinuity. It is important to note that PC and PMMA are nearly miscible, as shown recently.[15] The presence of MBS particles can greatly modify the rheological properties[14] and thereby favor such morphologies. Annealing at processing temperature (270°C) does not change the overall lo-

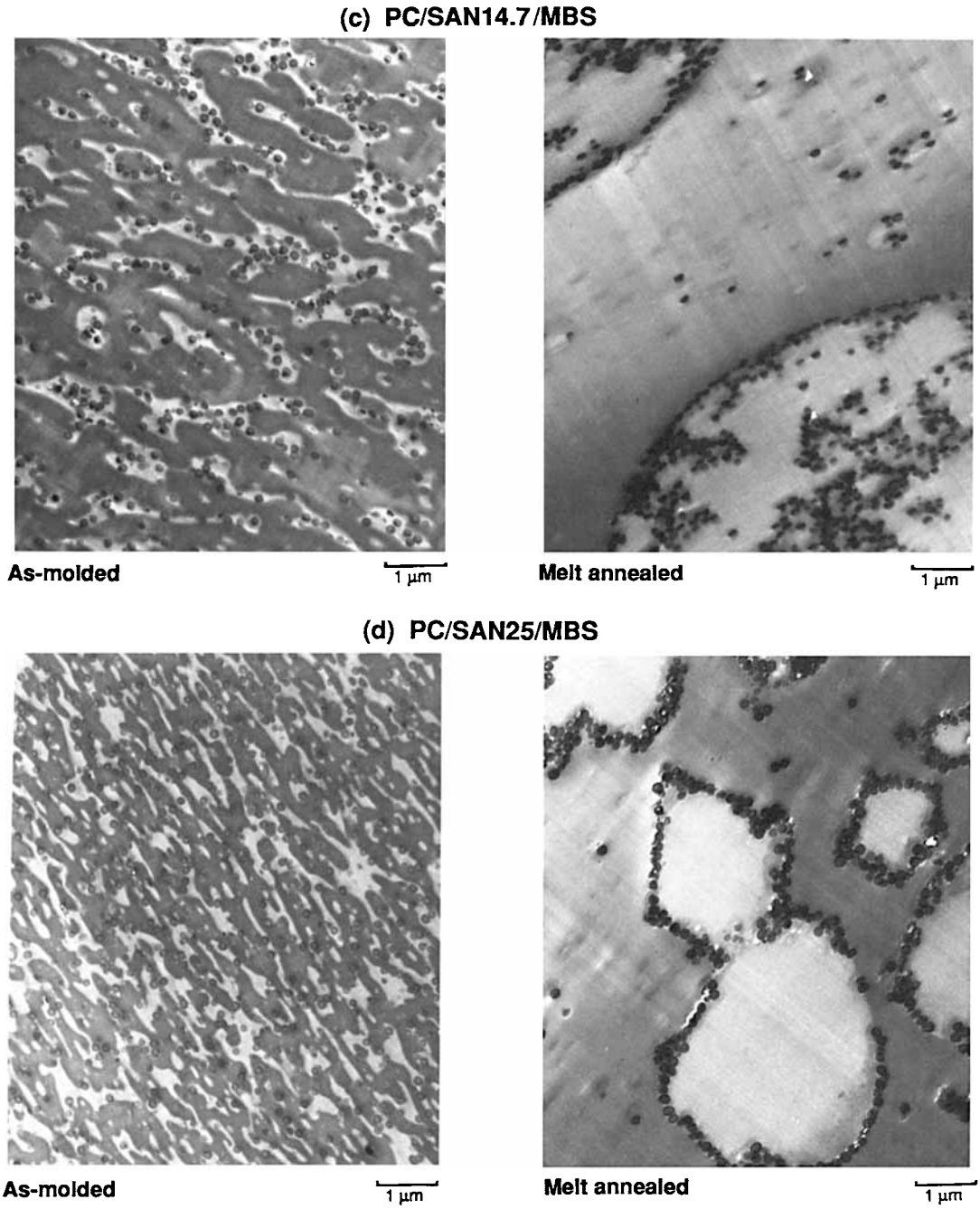

Figure 9 *(continued from previous page)*

cation of the MBS particles but does seem to cause them to undergo some agglomeration in the PMMA phase.

Ternary blends containing SAN14.7 show similar morphological behavior as ternary blends containing PMMA. The MBS particles tend to be located within the SAN14.7 phase in the as-molded blend, evidently because of the miscibility of their PMMA shell with this SAN.[16] After melt annealing, some MBS particles are located at the PC–SAN14.7 interface. An analysis of surface forces predicts the MBS particles to be located at the interface in this system at equilibrium. As found for PMMA, the tendency for PC–SAN14.7 cocontinuity appears to disintegrate during melt annealing.

For ternary blends containing PS, the MBS par-

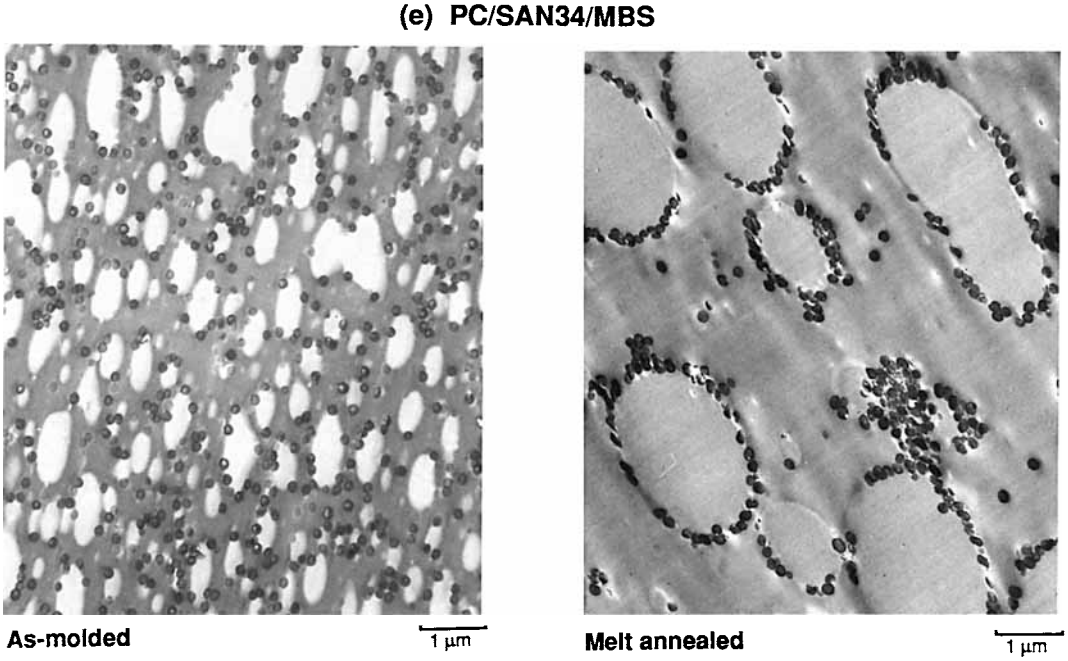

Figure 9 *(continued from previous page)*

ticles accumulate mostly at the PC–PS interface[26] and the PS domains appear to grow considerably due to particle retraction and coalescence during melt annealing. When the BP is SAN25, the PC–SAN25 cocontinuity tends to disintegrate and the MBS particles concentrate mainly at the PC–SAN25 interface. When SAN34 is the BP phase in the ternary blend, MBS particles concentrate at the PC–SAN34 interface while some agglomerate in the PC phase. In general, annealing tends to cause the distribution of MBS particles to become consistent with the equilibrium location predicted from surface force analysis as summarized in Table I and reported in detail elsewhere.[14]

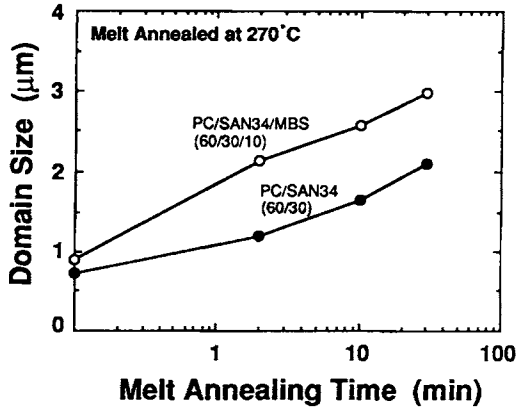

Figure 10 Comparison of growth of SAN34 domains in binary and ternary PC blends during melt annealing at 270°C.

Figure 10 compares the BP domain size in ternary PC/SAN34/MBS blends with the corresponding binary blends without MBS particles as a function of melt-annealing time. It is interesting that the SAN34 phase size always appears larger when MBS particles are present. The measure of domain size used here is the weight average dimension defined by eq. (4) where the dimension is the diameter of circular particles or the long dimension of elliptical particles [a few irregularly shaped particles were ignored—see Figs. 8 and 9(e)—for simplicity].

PROPERTY AND MORPHOLOGY RELATIONSHIPS

As-molded, ternary PC/BP/MBS blends were found to be quite tough. The least tough ternary system is the one based on BP = PS, which has an as-molded impact strength of 2.3 ft-lb/in. Figure 11 schematically summarizes the morphologies observed for these as-molded ternary blends and the changes that occur as a result of melt annealing at 270°C. Significant morphological changes occur

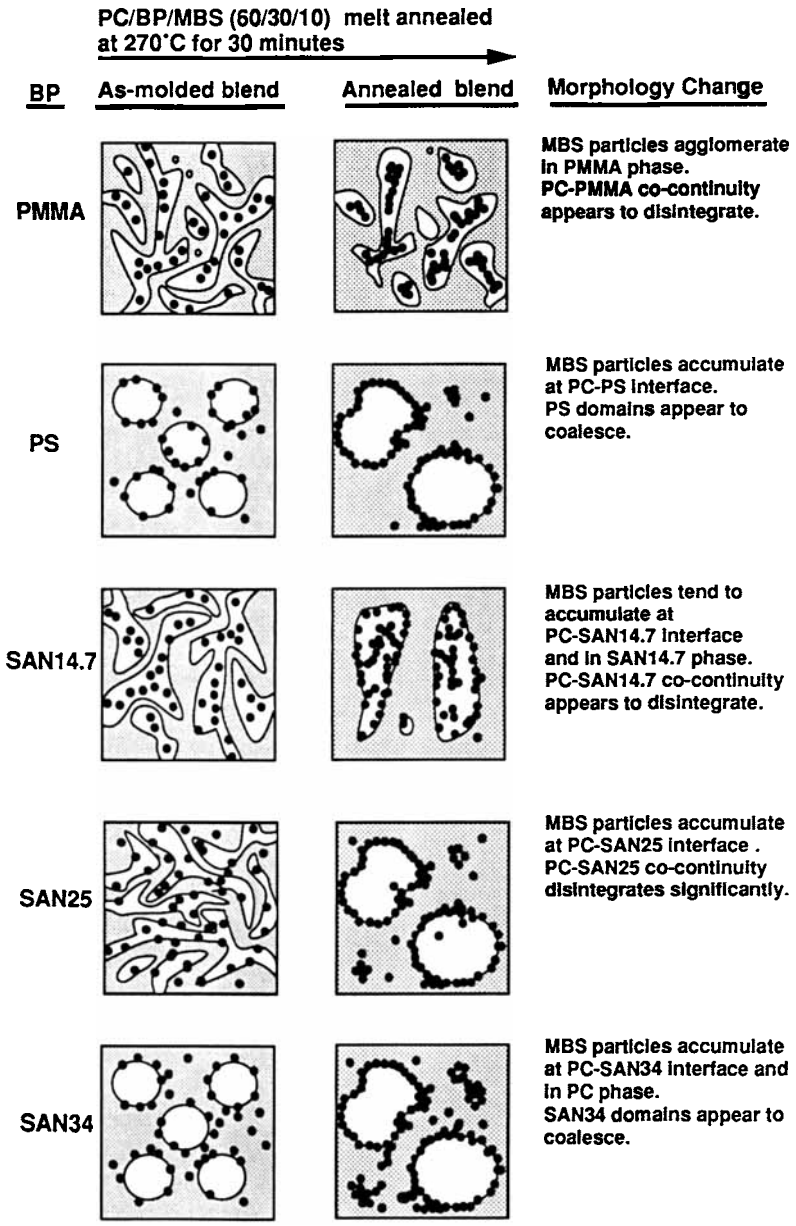

Figure 11 Schematic of morphology change of ternary PC/BP/MBS (60/30/10) blends due to melt annealing at 270°C for 30 min.

even after relatively short melt-annealing times. There are also corresponding changes in blend properties. Figure 12 shows the loss in impact strength for ternary blends when the BP is PMMA and SAN25. The least severe decline in toughness is seen for blends based on PMMA, while blends based on the other BPs become quite brittle after only 2 min of melt annealing at 270°C.

The profound changes that occur in the domain morphology during melt annealing are due to several factors. First, the relaxation of the highly oriented skin layer produces spherical BP particles. Second, in the core region dispersed particle coalescence and growth take place. Here, the relative viscosities of the component polymers and their interfacial energetics play a role. Figure 11 of ref. 14 gives comparative rheological information about the polymers used that indicated relatively small viscosity differ-

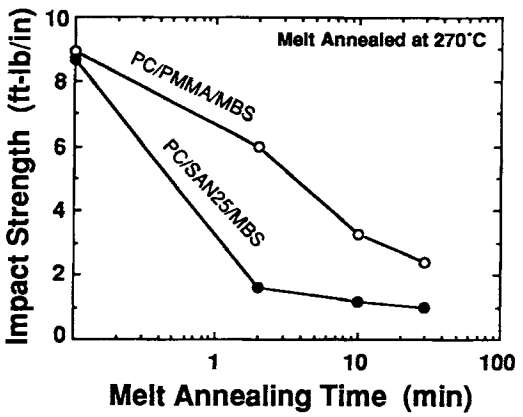

Figure 12 Notched Izod impact strength of PC/BP/MBS (60/30/10) blends as a result of melt annealing at 270°C.

ences between the BPs in comparison to PC and KM680. Surface energy effects have been pointed out by the data in Table 1.

To properly evaluate changes in mechanical properties that occur during melt annealing at 270°C, it is essential to understand the chemical stability of each of the blend components. In the absence of water and oxygen, PC is quite stable at 270°C for times much longer than those used here.[27,28] Likewise, PS and its copolymers with acrylonitrile should be adequately stable for the times and temperature of interest here.[29] PMMA, on the other hand, is noted for its tendency to depolymerize[27]; however, commercial grades like those used here are actually copolymers designed to mitigate this problem to some extent. A TGA trace shown in Figure 13(a) documents the behavior of the commercial PMMA used here. There is a small loss in mass of about 6% on isothermal heating at 270°C for 30 min followed by more severe decomposition at much higher temperatures. Note that noncommercial PMMA materials are generally much less stable.[30]

Figure 13(b) shows a TGA analysis of the MBS modifier. During holding at 270°C for 30 min, it loses only about 1.5% mass, most of which is probably MMA from the shell. A greater concern for the MBS modifier is thermal crosslinking of the butadiene-based rubber core.[29]

Dynamic mechanical analysis was used to more explicitly explore this aspect of the chemical stability of KM 680 at 270°C. Figure 14 shows the dynamic mechanical properties of as-molded KM 680 and after heating for 30 min at 270°C. There are some obvious changes in the dynamic mechanical properties that occur as a result of this heat history. It is significant to note that the temperature at which tan δ of the rubber peak reaches its maximum has shifted upward by only 7°C (from −61°C), indicating that the butadiene-based core remains elastomeric. Above the rubber phase T_g, the modulus remains as low if not lower than the as-molded modifier. These facts suggest that the various changes that occur at 270°C probably do not greatly impair the effectiveness of KM 680 to act as an impact modifier. In line with this, it is interesting to note in Table III that the properties of PC/MBS binary blends are only slightly changed by melt annealing. Accordingly, it appears that the dramatic changes in the ternary blend ductility are mostly caused by morphological changes during melt blending.

Only PC/PMMA/MBS blends maintain their toughness during the early stages of melt annealing (Table III and Fig. 12). The most obvious feature that distinguishes the PMMA-containing blend from the others is the extent to which the MBS particles migrate into the interfacial region during melt annealing. For blends based on PMMA, the MBS particles are entirely located in the PMMA phase and do not migrate to the interface during

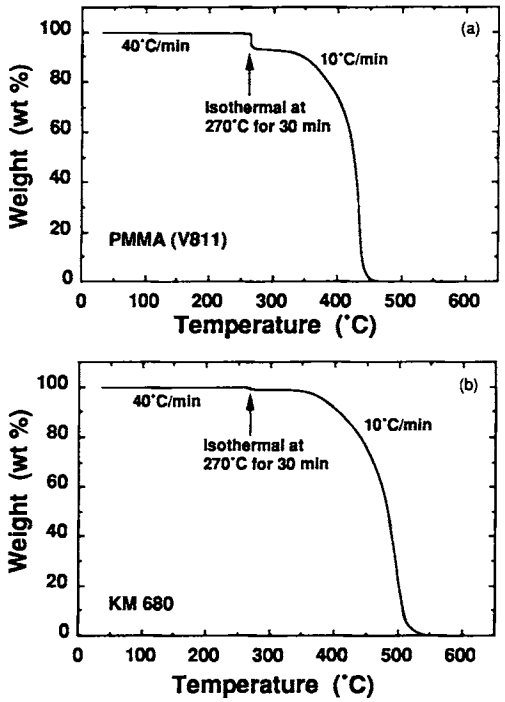

Figure 13 TGA traces of PMMA and KM 680. Samples were annealed at 270°C for 30 min in nitrogen, then heated at 10°C/min up to 600°C.

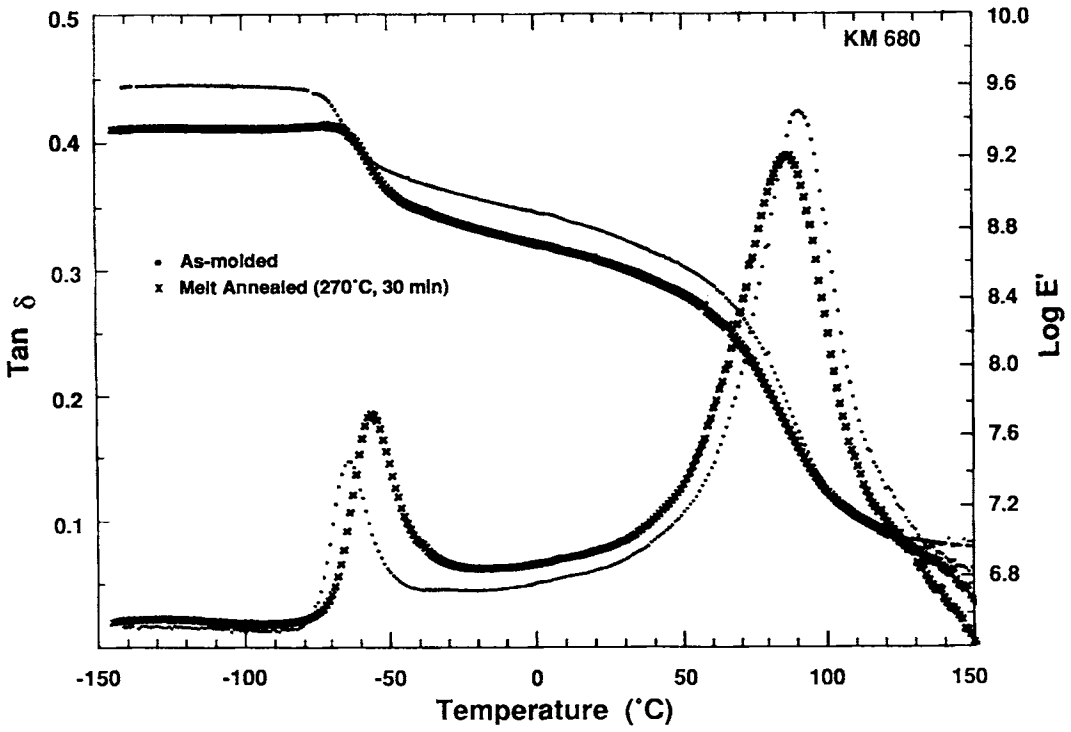

Figure 14 Dynamic mechanical properties of KM 680 as-molded and after melt annealing at 270°C for 30 min.

melt annealing. For ternary blends based on all other BPs, melt annealing causes significant migration of the MBS particles to the PC–BP interface. Apparently, location of the MBS particles at the PC–BP interface is undesirable for good toughness. This is an interesting observation since previous work showed that blends of high-impact PS and ABS have good toughness when similar PMMA-grafted rubber particles were located at the interface between them.[31] The absence of any toughening of the BP phase by MBS particles may be an important issue here.

Another factor that can influence properties is the change in morphology of the PC and BP phases that occurs during melt annealing. The consequences of this can be seen most clearly by examining the changes in morphology and ductility of binary blends. Such effects are illustrated in Figure 15 for PC/PS and PC/SAN25 blends. There is a reduction of notched Izod impact strength that occurs simultaneously with the growth of domain size for both systems. The decrease in impact strength for blends with PS is rapid. This is most probably due to the disappearance of the oriented skin layer of the molded bars and the poor interfacial adhesion of PS to PC. The changes in the PC/SAN25 blends are less dramatic, however. Overall, the as-molded binary blends with the smallest domain size distribution have the best impact strength.

CONCLUSIONS

Injection-molded binary blends of PC with a number of BPs and ternary blends containing an MBS modifier were annealed quiescently at 270°C to simulate conditions of no flow or low stress that may occur in molds, runners, and manifolds when these materials are melt processed. Changes in blend morphology and toughness were found to occur as a result of melt annealing.

A significant change in blend morphology occurs in less than 2 min of melt annealing at 270°C. In binary blends, the dispersed BP phase shows significant enlargement when viewed in the plane perpendicular to the flow direction. The ternary blends containing the MBS impact modifier also show apparent domain growth and other more complex behavior. For the ternary blends where the BP phase is PMMA, SAN14.7, or SAN25, the PC and BP

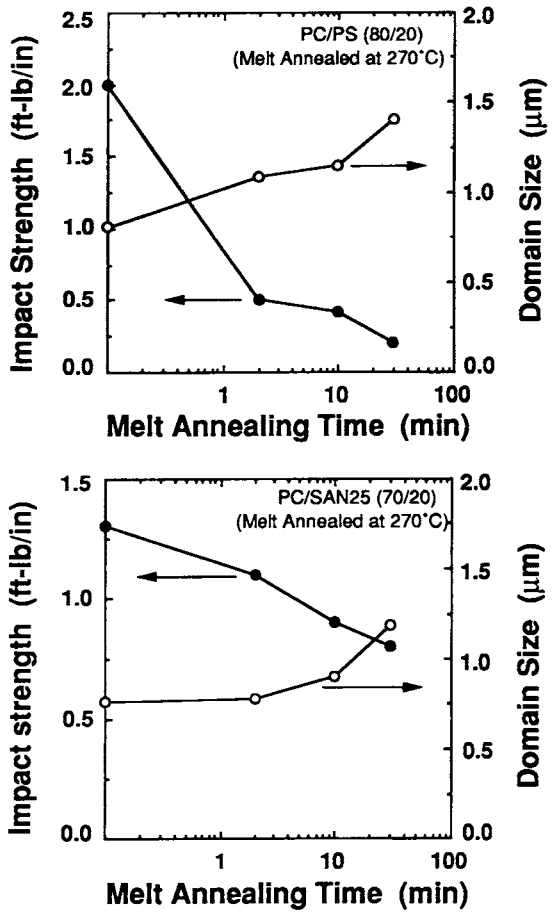

Figure 15 Relationship between change of domain size and Izod impact strength of binary PC blends after melt annealing at 270°C. (a), PC/PS (80/20); (b), PC/SAN25 (70/20).

phases tend to form cocontinuous structures in the as-molded materials. This cocontinuity is lost during melt annealing as the BP phase progressively becomes more spherical and grows in size. The location of the MBS particles may also change during melt annealing. When the dispersed phase is PMMA or SAN14.7, the MBS particles agglomerate but remain distributed in the BP phase. In all other cases, the MBS particles tend to relocate to the interface between PC and the BP phase. In the latter cases, the notched Izod impact strength is significantly reduced even after 2 min at 270°C. If the MBS particles remain in the BP phase, the loss of impact strength is much more gradual. Evidently, the abrupt loss in impact strength is primarily due to the depletion of the impact modifier in the brittle phase. The possible contributions of degradation of the polymeric components were also considered, but the experimental results indicate that the major reason for loss in toughness during melt annealing is morphological changes.

This research is based in part on work supported by the Texas Advanced Technology Program under Grant No. 066.

REFERENCES

1. D. R. Paul, J. W. Barlow, and H. Keskkula, in *Mark-Bikales-Overberger-Menges: Encyclopedia of Polymer Science and Engineering,* 2nd ed., John Wiley and Sons, New York, 1988, Vol. 12, p. 399.
2. C. D. Han, *Multiphase Flow in Polymer Processing,* Academic Press, New York, 1981.
3. S. Wu, *Polym. Engng. Sci.,* **27,** 335 (1987).
4. B. D. Favis, *J. Appl. Polym. Sci.,* **39,** 285 (1990).
5. C. Chen, E. Fontan, K. Min, and J. L. White, *SPE Tech. Papers,* **46,** 1127 (1988).
6. J. L. White and K. Min, *Makromol. Chem., Macromol. Symp.,* **16,** 19 (1988).
7. D. Quintens, G. Groeninckx, M. Guest, and L. Aerts, *Polym. Engng. Sci.,* **30,** 1484 (1990).
8. D. Quintens, G. Groeninckx, M. Guest, and L. Aerts, *Polym. Engng. Sci.,* **30,** 1474 (1990).
9. B. Z. Jang, D. R. Uhlmann, and J. B. Vander Sande, *Rubber Chem. Tech.,* **57,** 291 (1984).
10. I. Fortelny and J. Kovar, *Polym. Composites,* **9,** 119 (1988).
11. D. Freitag, U. Grigo, P. R. Muller, and W. Nouvertne, in *Mark-Bikales-Overberger-Menges: Encyclopedia of Polymer Science and Engineering,* 2nd ed., John Wiley and Sons, New York, 1988, Vol. 11, p. 648.
12. E. A. Joseph, D. R. Paul, and J. W. Barlow, *J. Appl. Polym. Sci.,* **27,** 4807 (1982).
13. T. W. Cheng, H. Keskkula, and D. R. Paul, *J. Appl. Polym. Sci.* (to appear).
14. T. W. Cheng, H. Keskkula, and D. R. Paul, *Polymer* (to appear).
15. M. Nishimoto, H. Keskkula, and D. R. Paul, *Polymer,* **32,** 273 (1991).
16. M. E. Fowler, J. W. Barlow, and D. R. Paul, *Polymer,* **28,** 1177 (1987).
17. W. D. Harkins, *The Physical Chemistry of Surface Films,* Reinhold Pub. Co., New York, 1952, p. 23.
18. S. Y. Hobbs, M. E. J. Dekkers, and V. H. Watkins, *Polymer,* **29,** 1589 (1988).
19. T. D. Goldman, U.S. Pat. 4,443,585 (April 17, 1984) (to Rohm and Haas Co.).
20. J. S. Trent, J. I. Scheinbeim, and P. R. Couchman, *Macromolecules,* **16,** 589 (1983).
21. G. C. Eastmond and E. G. Smith, *Polymer,* **14,** 509 (1973).

22. J. D. Keitz, J. W. Barlow, and D. R. Paul, *J. Appl. Polym. Sci.*, **29,** 3131 (1984).
23. T. Kunori and P. H. Geil, *J. Macromol. Sci.-Phys.*, **B18**(1), 93 (1980).
24. A. J. Oshinski, H. Keskkula, and D. R. Paul, *Polymer* (to appear).
25. M. E. Fowler, H. Keskkula, and D. R. Paul, *Polymer,* **28,** 1703 (1987).
26. M. E. Fowler, H. Keskkula, and D. R. Paul, *J. Appl. Polym. Sci.*, **37,** 225 (1989).
27. D. J. Carlsson and D. M. Wiles, in *Mark-Bikales-Overberger-Menges: Encyclopedia of Polymer Science and Engineering,* 2nd ed., John Wiley and Sons, New York, 1988, Chap. 4, p. 678.
28. A. Davis and J. H. Golden, *J. Macromol. Sci.-Revs. Macromol. Chem.*, **C3**(1), 49 (1969).
29. K. McCreedy and H. Keskkula, *Polymer,* **20,** 1155 (1979).
30. A. Rincon and I. C. McNeill, *Polym. Degrad. Stab.*, **18,** 99 (1987).
31. H. Keskkula, D. R. Paul, K. M. McCreedy, and D. E. Henton, *Polymer,* **28,** 2063 (1987).

Received January 29, 1991
Accepted August 16, 1991